

Effects of divalent cations on phase behavior and structure of a zwitterionic phospholipid (DMPC) monolayer at the air-water interface

Sumit Kewalramani,¹ Htay Hlaing,^{1,2} Benjamin M. Ocko,¹ Ivan Kuzmenko,³ and Masafumi Fukuto^{1*}

¹Condensed Matter Physics and Materials Science Department, Brookhaven National Laboratory, Upton, NY 11973

²Department of Physics and Astronomy, Stony Brook University, NY 11794

³X-ray Science Division, Advanced Photon Source, Argonne National Laboratory, Argonne, IL 60439

*To whom correspondence should be addressed. E-mail: fukuto@bnl.gov.

Effect of ion concentration on the lipid phase behavior

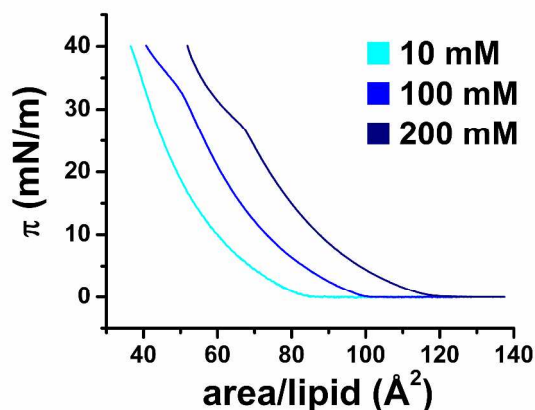


Figure S1. Surface pressure-area isotherms for a DMPC monolayer spread on aqueous solutions (10 mM MES, pH 6) of zinc chloride at 3 different concentrations, measured at $T = 22.5\text{ }^\circ\text{C}$ (as opposed to $15\text{ }^\circ\text{C}$ in Fig 1, main text). The isotherms for 100 and 200 mM ZnCl_2 have been shifted along the area axis by 10 and 20 \AA^2 , respectively, for clarity.

As described in the main text, the presence of divalent cations lowers the surface pressure π_C at the onset of the LE-L₂ transition. Zn^{2+} lowers π_C the most, followed by Ca^{2+} , Mg^{2+} , and Ni^{2+} . In addition to the dependence on the specific cation present, the

transition pressure also depends upon the concentration of the ion in the aqueous subphase. Figure S1 shows π - A isotherms of DMPC on Zn^{2+} solutions of different concentrations (measured at 22.5 °C, instead of 15 °C for the isotherms in Fig 1 of the main text). The data show that π_C decreases with increasing concentration of the divalent cation. According to the “local binding model,”¹ the ratio of the ion-bound lipid to the free lipid is directly proportional to the concentration of the cation. This implies that the more ions bind to the lipid monolayer, the lower π_C is. Taken together, the observed specific-cation and concentration effects on the transition pressure indicate that the binding affinities for the divalent cations with the lipid headgroup follows the sequence $\text{Zn}^{2+} > \text{Ca}^{2+} > \text{Mg}^{2+} > \text{Ni}^{2+}$. This sequence is consistent with the affinity sequence based on previous measurements on bilayers (vesicles and multilayers).^{2, 3}

Additional GID data from a DMPC monolayer in the presence of Ca^{2+} , Mg^{2+} or Ni^{2+} .

GID data from a DMPC monolayer on a 150 mM solution of Ca^{2+} , Mg^{2+} , or Ni^{2+} at π - $\pi_C \sim 17$ mN/m (Figure 2, top) show 2 diffraction peaks, an in-plane peak and a doubly degenerate out-of-plane peak. The peak positions are nearly identical for the three cases: the in-plane diffraction peak lies at $q_{xy} \sim 1.45 \text{ \AA}^{-1}$, and the out-of plane peak is centered at $q_{xy} \sim 1.38 \text{ \AA}^{-1}$ and $q_z \sim 0.5 \text{ \AA}^{-1}$. This implies that at π - $\pi_C \sim 17$ mN/m, the packing parameters of the DMPC alkyl tails, i.e., the 2D lattice parameters and the mean tilt angle of the lipid tails, are very similar for all three ions. In general, at a given π - π_C , the packing parameters for the lipid tails are identical for Ni^{2+} , Mg^{2+} , and Ca^{2+} (main text).

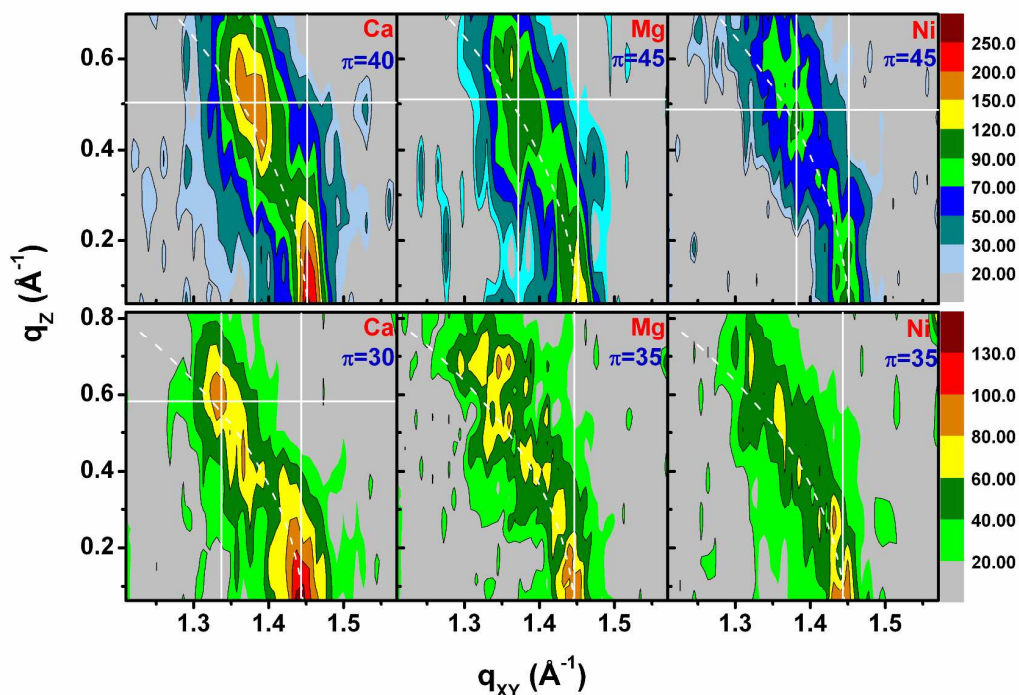


Figure S2. GID data from a DMPC monolayer on aqueous solutions (10 mM MES, pH 6) with 150 mM of Ca^{2+} (left), Mg^{2+} (center), and Ni^{2+} (right) collected at $T=15^\circ\text{C}$, and at excess surface pressures ($\pi - \pi_C$) of ~ 17 mN/m (top), and ~ 7 mN/m (bottom).

Despite the commonalities between Ni^{2+} , Mg^{2+} , and Ca^{2+} , there are some differences also. GID data collected at $\pi - \pi_C \sim 7$ mN/m (Figure S2, bottom) show that for Ca^{2+} , the out-of-plane peak is located in a narrow Δq_z range. GID data collected from DMPC in the presence of Zn^{2+} also displays a well defined out-of-plane peak at all surface pressures (main text). This implies that for Zn^{2+} and Ca^{2+} the width of the distribution in the tilt angle of the lipid tails is very narrow. By contrast, at $\pi - \pi_C \sim 7$ mN/m (Figure S2, bottom), the out-of-plane peak for Mg^{2+} and for Ni^{2+} appears smeared out along a “Scherrer” ring at $q = (q_{xy}^2 + q_z^2)^{1/2} \sim 1.45 \text{ \AA}^{-1}$, indicating a large distribution in the tilt angle of the alkyl tails. These observations suggest that ions with higher binding

affinities for the lipid headgroup induce better orientational ordering of the lipid alkyl tails than the ions which interact weakly with the lipid headgroups.

XR measurements

XR data were collected from both the LE and L₂ phases of DMPC on 150 mM salt solutions. Figure S3 (a) shows XR data normalized to the Fresnel reflectivity of an ideally flat aqueous subphase (symbols) as a function of q_z , for DMPC on a 150 mM solution of Zn²⁺. The data show that the position of the minima in the R/R_F curves shifts toward lower q_z values with increasing surface pressures. The first minimum position $q_{z\min}$ is related to the thickness of the monolayer as $2q_{z\min} \sim 3\pi(L_t+L_h/2)^{-1}$,^{4,5} where L_t is the thickness of the lipid alkyl tail sublayer, and L_h is the thickness of the lipid headgroup sublayer. Therefore, the lowering of $q_{z\min}$ with π implies that the lipid film gets thicker with increasing π . The position $q_{z\min} \sim 0.25 \text{ \AA}^{-1}$ observed at $\pi = 40 \text{ mN/m}$, gives $L_t+L_h/2 \sim 19 \text{ \AA}$. The thickness of the lipid tail at $\pi = 40 \text{ mN/m}$ is expected to be $L_t \sim 15.8 \text{ \AA}$, because the length of the alkyl tails in *all-trans* configuration along the tail axis is $\sim 16.7 \text{ \AA}$,⁶ and the tilt angle of the alkyl tails with respect to surface normal is $\sim 19^\circ$ (from GID data). The thickness of the lipid headgroup in the L₂ phase is expected to be $L_h \sim 7\text{-}8 \text{ \AA}$.⁶ Therefore, the expected value of $L_t+L_h/2$ at $\pi = 40 \text{ mN/m}$ is $\sim 19.5 \text{ \AA}$. This value is closely matched by $L_t+L_h/2=19 \text{ \AA}$ obtained from the position of the first minimum in the XR curve. Data with similar characteristics are obtained from DMPC on other salt solutions.

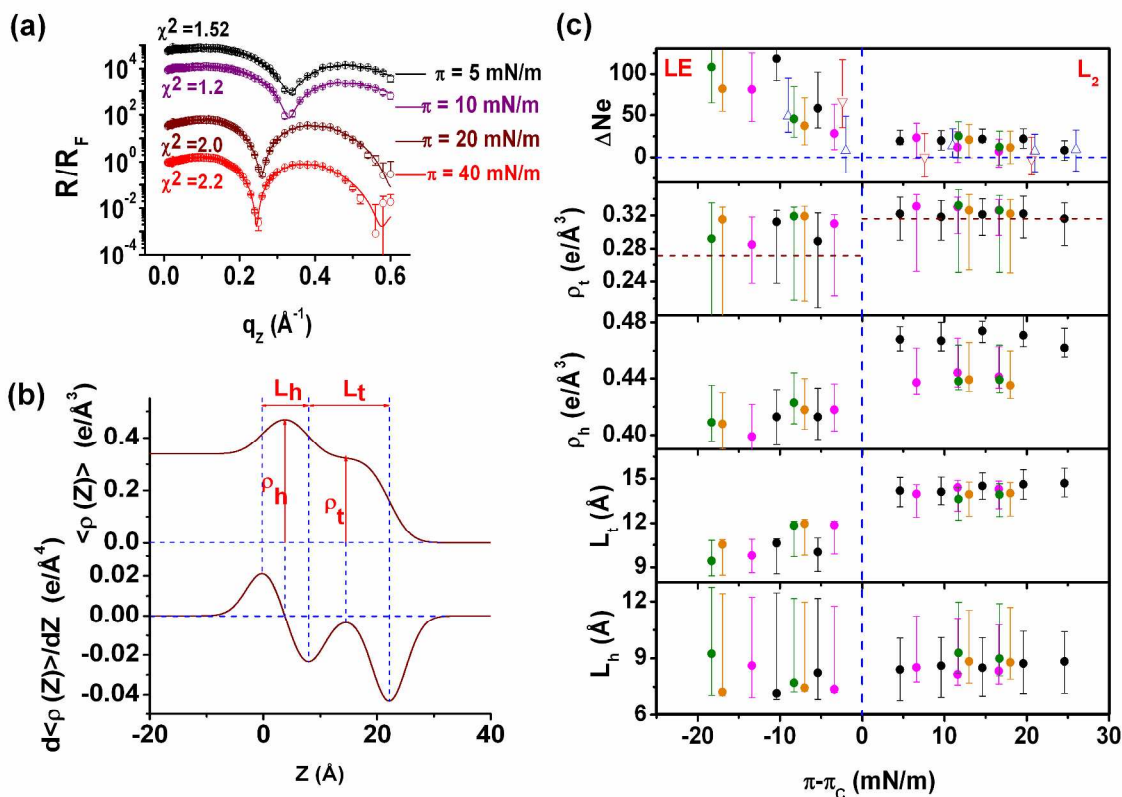


Figure S3. Summary of XR results. (a) Representative XR data, shown as the Fresnel-normalized reflectivity as a function of q_z , for DMPC monolayers on aqueous solutions (10 mM MES, pH 6) of 150 mM Zn^{2+} at $T = 15$ °C and $\pi = 5$ (top), 10, 20, and 40 mN/m (bottom). (b) Schematic representation of a 2-box electron density profile along the surface normal, its derivative, and the definitions of density-profile-determined parameters. (c) The excess-pressure dependence of the profile-derived parameters: the thickness of the headgroup and tail sublayers (L_h , L_t), electron density of the sublayers (ρ_h , ρ_t), and the excess electrons associated with the monolayer (ΔN_e). Filled symbols refer to DMPC monolayers on aqueous solutions (10 mM MES, pH 6) of different cations at $T = 15$ °C: Ni^{2+} (green), Mg^{2+} (orange), Ca^{2+} (magenta), and Zn^{2+} (black). The open triangles for ΔN_e represent DPPC monolayers on pure water at $T = 21$ °C (red) and 26 °C (blue).

The fitting of the XR data was carried out by using the standard “box” model for the average electron density profile $\langle\rho(z)\rangle$,⁷ which is based on the combination of error functions. To construct the model profile $\langle\rho(z)\rangle$, the DMPC monolayer between the aqueous subphase ($\langle\rho_{sub}\rangle = 0.334 \text{ e}/\text{\AA}^3$ for Ca^{2+} , $0.334 \text{ e}/\text{\AA}^3$ for Mg^{2+} , $0.344 \text{ e}/\text{\AA}^3$ for Ni^{2+} , and $0.338 \text{ e}/\text{\AA}^3$ for Zn^{2+}) and the vapor ($\langle\rho\rangle = 0$) was represented by two slabs which correspond to the lipid headgroup (h) and the alkyl tail (t) sublayers. The parameters that defined the model $\langle\rho(z)\rangle$ were the electron densities of the two boxes (ρ_1 and ρ_2), their thicknesses (L_1 and L_2), and a common Gaussian roughness parameter σ for the three interfaces. The reflectivity corresponding to this model density profile was calculated by the matrix method of Parratt formalism^{8, 9} for $q_z < 0.1 \text{ \AA}^{-1}$ and using the kinematic (Born) approximation for $q_z \geq 0.1 \text{ \AA}^{-1}$. The calculated reflectivity was fitted to the experimental data for $q_z \geq 0.05 \text{ \AA}^{-1}$ by varying the box parameters. The best fits for the data from DMPC on a 150 mM Zn^{2+} solution are shown in Figure S3(a) as solid lines. The χ^2 values shown in the figure are representative of the quality of fits obtained for all data. The box parameters that generated the fits were found to be strongly coupled, such that vastly varying sets of parameters could generate similar density profiles and hence similar fits to the data. It should be noted that XR depends only on the profile $\langle\rho(z)\rangle$ as a whole and not on how it is constructed. Therefore, physically meaningful quantities that characterize the monolayer were extracted from the extremum positions in the best-fit electron density profile and its derivative.¹⁰ The definitions of these quantities are provided in Figure S3(b), and the profile-derived quantities for DMPC on all salt solutions are plotted as a function of the excess surface pressure $\pi - \pi_C$ in Figure S3(c). The uncertainties on the profile-derived quantities were estimated from the profiles

defined by sets of box-model parameters on $\Delta\chi^2 \sim 1$ (68% confidence limit) contours. In order to include the effects of parameter correlations, the $\Delta\chi^2 \sim 1$ contours had been obtained by varying all the fitted box-model parameters simultaneously.

The uncertainties associated with the thickness L_h of the headgroup sublayer are rather large. However, the obtained best-fit values were found to be within the physically permissible range for the thickness of the headgroup layer, 5-9 Å,⁶ as determined by molecular models. In the L_2 phase, the thickness of the lipid tail (L_t) is independent of the specific cation present. By contrast, the electron density for the lipid headgroup (ρ_h) is consistently higher in the presence of Zn^{2+} than for other ions. These ion-independent and specific-ion effects are discussed in detail in the main text. The extracted electron densities for the lipid tails (ρ_t) have large associated uncertainties. However, the best fit values lie very close to the expected electron densities of $0.27 \text{ e}/\text{Å}^3$ in the LE phase, and $0.316 \text{ e}/\text{Å}^3$ in the L_2 phase (dashed lines).¹⁰

The above XR analysis has also been used to estimate the number of excess electrons per lipid, ΔN_e , associated with the lipid monolayer. Shown in the top panel of Fig. S3(c) is $\Delta N_e = (L_h\rho_h + L_t\rho_t)A - N_L$, where A is the isotherm-based area/lipid for the LE phase and the GID-based area/lipid (A_x) for the L_2 phase, and N_L is the number of electrons per lipid molecule.

For lipids on pure water, the excess electrons ($\Delta N_e > 0$) arise solely from the headgroup hydration. As explained in Experimental Methods, problems with film stability prevented X-ray measurements on DMPC monolayers on pure water (or on a salt-free MES solution). As an alternative control, we collected XR data from DPPC monolayers on pure water, which were stable. Figure S3(c) shows that the estimated

values of ΔN_e for DPPC on water (open triangles) are much higher in the LE phase than in the L_2 phase, indicating dehydration of the PC headgroup upon the LE-to- L_2 transition. This inference is qualitatively consistent with previously published results.^{11, 12} However, the corresponding number of water molecules associated with the lipid headgroup in the L_2 phase, found to be $N_w = \Delta N_e/10 = 1 \pm 2$ per lipid at $T = 26^\circ\text{C}$ and at $\pi = 40$ mN/m, is lower than the previously published values of $N_w = 4 \pm 2.5$ ¹³ and 4 ± 1 .¹¹ We cannot currently explain the origin of these discrepancies. However, we note that our estimate of N_w for the L_2 -phase monolayer of DPPC is similar to the previously reported value of $N_w = 1.75 \pm 1.25$ for the gel phase of DPPC bilayers.¹⁴

For DMPC monolayers on salt solutions, the excess electrons may originate from ion-lipid binding and/or the headgroup hydration. Figure 3(c) shows that ΔN_e estimated for DMPC in the presence of divalent cations (filled circles) is, again, much higher in the LE phase than in the L_2 phase. However, for the LE phase, the excess electrons are attributed largely to the hydration of the lipid headgroup, for two reasons. First, the large values of ΔN_e in the LE phase are comparable to those for DPPC on pure water (open triangles). Second, on the basis on previous results on lipid multibilayers, divalent cations are expected to bind to lipids primarily in the L_2 phase.¹⁵ For the L_2 phase, the contribution of water to ΔN_e is expected to be small because of the dehydration of the lipid headgroups upon the LE- L_2 transition, as discussed above. The contribution to ΔN_e from ion-lipid binding should also be small because the metal ions used in the current study have relatively low atomic numbers. For example, even if the metal ions were to bind to all the lipids in a 1:1 stoichiometric ratio, the ion contribution to ΔN_e would only range from 30 for Zn to 12 for Mg. Consistent with these expectations, the XR-derived

values of ΔN_e for the L_2 phase are small (~ 20). However, because of the large uncertainties associated with ΔN_e (± 10 for DMPC on salt solutions, ± 20 for DPPC on pure water), it has not been possible to quantify the extent of ion-lipid binding in the L_2 phase.

It should be noted that the above limitation in determining ΔN_e in no way implies the absence of cations at the interface. As discussed in the main text, the observed ion-specific effects provide indirect evidence that divalent cations are present at the interface and do interact with the DMPC monolayer in the L_2 phase.

Effects of baked vs. unbaked salts

For Langmuir monolayers even small amounts of interface-active organic impurities can drastically affect the stability, phase behavior, and structure of the monolayer. It was recently reported that even “ultrapure” grade inorganic salts from commercial vendors contain non-negligible quantities of organic impurities.¹⁶ However, the same study reported that baking of salts at 300-350°C for a few hours reduced these organic impurities. To ensure that our observations do not contain artifacts due to the presence of such impurities, we have studied the effects of both baked and unbaked salts on the DMPC monolayer.

Surface pressure-area isotherm measurements for DMPC on metal chloride solutions show that the transition pressure π_C is independent of whether the salts are baked or unbaked (data not shown). However, for unbaked salts, the LE- L_2 coexistence region in the isotherm was found to be more smeared out than for baked salts. Nevertheless, these observations indicate that the π_C values used in our analysis are fairly

robust. We also found that the isotherms for DMPC on the solutions of baked salts were unaffected by whether or not the solution was filtered through a 0.2 μm surfactant free cellulose acetate membrane.

For a given lipid monolayer, the time required to perform X-ray scattering measurements at 4-5 different surface pressures was ~ 8 hrs. To test the integrity of the DMPC monolayer over time, we performed time-dependent X-ray measurements at a few chosen surface pressures. For the L_2 phase, regardless of whether salts were baked or unbaked, GID and XR data were found to be very reproducible over a period of > 8 hrs. By contrast, for the LE phase, the first minima in the XR curves were found to shift continuously towards lower q_z values with increasing time. This effect was more pronounced for unbaked salts. For example, at $\pi=10$ mN/m for a DMPC monolayer on a 150 mM ZnCl_2 solution, the first minimum in the XR curve showed a shift of $\Delta q_z \sim -0.02 \text{ \AA}^{-1}$ after ~ 6 hrs, when unbaked salt was used. A much smaller shift of $\Delta q_z < -0.01 \text{ \AA}^{-1}$ after ~ 8 hrs was observed for baked salts. Therefore, it appears that the organic impurities contained in the salt solutions diffuse to the liquid-vapor interface slowly over time, and are miscible with the LE phase monolayer. The adsorption of these impurities at the interface increases the apparent thickness of the lipid film in the LE phase. Further, these observations suggest that the baking of salts significantly reduces the organic impurities. Therefore, for the LE phase, we have used data that were collected from films prepared with baked salts and taken within 3 hrs after spreading the monolayer.

References

- (1) Leontidis, E.; Aroti, A.; Belloni, L. Liquid Expanded Monolayers of Lipids as Model Systems to Understand Anionic Hofmeister Series: 1. A Tale of Models. *J. Phys. Chem. B*, **2009**, *5*, 1447-1459.
- (2) Tatulian, S. A. Binding of Alkaline-Earth Metal Cations and some Anions to Phosphatidylcholine Liposomes. *Eur. J. Biochem.* **1987**, *170*, 413-420.
- (3) McLaughlin, A.; Grathwohl, C.; and McLaughlin, S. The Adsorption of Divalent Cations to Phosphatidylcholine Bilayer Membranes *Biochim. Biophys. Acta* **1978**, *513*, 338-357.
- (4) Kjaer, K.; Als-Nielsen, J.; Helm, C. A.; Tippmann-Krayer, P.; Möhwald, H. An X-Ray-Scattering Study of Lipid Monolayers at the Air-Water Interface and on Solid Supports. *Thin Solid Films*, **1988**, *159*, 17-28.
- (5) Kjaer, K.; Als-Nielsen, J.; Helm, C. A.; Tippman-Krayer, P.; and Möhwald, H. Synchrotron X-ray Diffraction and Reflection Studies of Arachidic Acid Monolayers at the Air-Water interface. *J. Phys. Chem.* **1989**, *93*, 3200.
- (6) Helm, C. A.; Möhwald, H; Kjaer, K.; Als-Nielsen, J. Phospholipid Monolayer Density Distribution Perpendicular to the Water Surface. A Synchrotron X-Ray Reflectivity Study. *Europhys Lett.*, **1987**, *4*, 697.
- (7) Als-Nielsen, J.; McMorrow, D., *Elements of Modern X-ray Physics*. Wiley: Chichester, 2001.
- (8) Parratt, L. G. Surface Studies of Solids by Total Reflection of X-rays. *Physical Review* **1954**, *95*, 359.
- (9) Lekner, J. *Theory of Reflection*. Dordrecht, Martin Nijhoff Publishers: Hingham, MA, USA, 1987.
- (10) Fukuto, M; Heilmann, R. K.; Pershan, P. S.; Yu, S. J. M.; Soto, C. M.; Tirrell, D. A. Internal Segregation and Side Chain Ordering in Hairy-Rod Polypeptide Monolayers at the Gas/Water Interface: An X-Ray Scattering Study. *J. Chem. Phys.* **2003**, *119*, 6253-6270.
- (11) Naumann, C.; Brumm, T.; Rennie, A, R.; Penfold, J.; Bayerl, T. M. Hydration of DPPC Monolayers at the Air/Water Interface and Its Modulation by the Nonionic Surfactant C12E4: A Neutron Reflection Study. *Langmuir* **1995**, *11*, 3948.

-
- (12) Ma, G.; and Allen, H. C. DPPC Langmuir Monolayer at the Air-Water Interface: Probing the Tail and Head Groups by Vibrational Sum Frequency Generation Spectroscopy *Langmuir* **2006**, *22*, 5341.
- (13) Vaknin, D.; Kjaer, K.; Als-Nielsen, J.; and Lösche, M. Structural Properties of Phosphatidylcholine in a Monolayer at the Air-Water Interface. *Biophys. J.* **1991**, *59*, 1325.
- (14) Wiener, M. C.; Suter, R. M. ; Nagle, J. F. Structure of the Fully Hydrated Gel Phase of Dipalmitoylphosphatidylcholine *Biophys J.* **1989**, *55*, 315-325.
- (15) Binder, H.; Zschörnig, O. The Effect of Metal Cations on the Phase Behavior and Hydration Characteristics of Phospholipid Membranes. *Chem. Phys. Lipids* **2002**, *115*, 39-61
- (16) Sloutskin, E; Baumert, J; Ocko, B. M.; Kuzmenko, I; Checco, A; Tamam, L; Oler, L; Gog, T; Gang, O; Deutsch, M. The Surface Structure of Concentrated Aqueous Salt Solutions. *J. Chem. Phys.* **2007**, *126*, 054704.